JGR Atmospheres

RESEARCH ARTICLE
10.1029/2018JD029807

Key Points:
- We decompose soil moisture (SM)-evapotranspiration (ET) coupling into terms attributable to the different ET components
- Part of SM-ET coupling reflects the noncausal, positive correlation of soil moisture with canopy interception
- Projected increases in SM-ET coupling in regions of precipitation increase reflect the greater role of canopy interception

Supporting Information:
- Supporting Information S1

Correspondence to:
A. Berg,
ab5@princeton.edu

Citation:
Berg, A., & Sheffield, J. (2019). Historic and projected changes in coupling between soil moisture and evapotranspiration (ET) in CMIP5 models confounded by the role of different ET components. *Journal of Geophysical Research: Atmospheres*, *124*, 5791–5806. https://doi.org/10.1029/2018JD029807

Received 10 OCT 2018
Accepted 26 APR 2019
Accepted article online 2 MAY 2019
Published online 7 JUN 2019

Historic and Projected Changes in Coupling Between Soil Moisture and Evapotranspiration (ET) in CMIP5 Models Confounded by the Role of Different ET Components

Alexis Berg[1] and Justin Sheffield[2]

[1]Department of Civil and Environmental Engineering, Princeton University, Princeton, NJ, USA, [2]School of Geography and Environmental Science, University of Southampton, Southampton, UK

Abstract The coupling of soil moisture (SM) and evapotranspiration (ET) is a critical process of the terrestrial climate and water cycle, whose simulation in climate models exhibits substantial uncertainties. Here we investigate, across phase 5 of the Coupled Model Intercomparison Project models in present-day and future simulations, how this coupling manifests itself across the different components of ET: soil evaporation, transpiration, and canopy interception. We characterize summertime SM-ET coupling by (interannual) correlations, which we decompose into terms attributable to each ET component. The transpiration and soil evaporation terms share similar spatial patterns, but the contribution of transpiration, globally, is less positive. Canopy interception contributes a positive term to SM-ET coupling, reflecting the noncausal, rainfall-forced positive correlation between SM and canopy interception. Model differences are greatest for the transpiration term, which explains most of the model spread in SM-ET coupling. Models project a robust pattern of more positive SM-ET correlations in the future. In parts of the midlatitudes and Tropics, this increase reflects reduced precipitation and increased SM limitation on transpiration and soil evaporation. However, at higher latitudes (north of 50°N), increased SM-ET coupling is driven by the increased contribution of canopy interception induced by the increase in vegetation and precipitation. Analysis of ET partitioning is thus essential to the interpretation of simulated changes in ET and its drivers: While increased SM-ET correlations may suggest a widespread increase in SM limitation on ET in a warmer world, increases in actual SM control on land-atmosphere water fluxes are generally limited to regions of negative precipitation change.

1. Introduction

Interactions between the land surface and the overlying atmosphere are a key set of physical processes affecting surface climate over land. On various spatial and temporal scales, land surface biophysical characteristics, such as moisture availability, albedo, and surface roughness, vary in response to atmospheric forcing in terms of moisture (precipitation) and energy (radiation); in turn, these variations modulate land-atmosphere exchanges of water and energy, which modulate surface climate characteristics, such as near-surface air temperature, humidity, boundary layer profiles, and precipitation occurrence. Correct representation of these processes in numerical climate models is essential for realistic simulations of the climate system, in particular over land. Simulating land-atmosphere fluxes and their interaction with surface climate is the primary role of the land surface models embedded in climate models (Dirmeyer, 2018).

On time scales from intraseasonal to interannual, soil moisture (SM) is the dominant land surface state variable affecting the global atmosphere (Dirmeyer, 2011b). SM availability in particular regulates the partitioning of available energy at the surface into latent and sensible heat fluxes. The resulting coupling between SM and the atmosphere affects climate in numerous ways (e.g., Seneviratne et al., 2010). The control of SM on the latent heat flux, or evapotranspiration (ET), is often referred to as the "terrestrial leg" of that coupling (Dirmeyer, 2011a): It is the first link in a chain of processes whereby variations in SM impact on various surface climate variables. As such, SM-ET coupling is a critical process that needs to be represented accurately in climate models. Because part of ET occurs through vegetation and is coupled to photosynthesis, it is also a critical process for Earth System Model simulations of the coupled carbon cycle-climate system.

Due to the complexity of the land-atmosphere interface, the historical lack of extensive observational constraints on land-atmosphere exchanges and the terrestrial water cycle, and the different modeling choices made in the representation and parameterization of land surface processes, climate models show large differences in their simulation of land-atmosphere fluxes, including ET (e.g., Mueller & Seneviratne, 2014, and references therein). This extends to uncertainties in the physical drivers of these fluxes, including the role of SM limitation. For instance, in the context of the landmark Global Land-Atmosphere Coupling Experiment (Koster et al., 2004), Koster et al. (2006) showed that models display large differences in the patterns and amplitude of SM-atmosphere coupling, with most of the model spread linked to differences in the terrestrial leg (Guo et al., 2006). Dirmeyer et al. (2006) also highlighted the differences between Global Land-Atmosphere Coupling Experiment models in the functional shape and strength of the relationship between soil wetness and ET. More recently, Berg and Sheffield (2018a) analyzed the diversity of models of the phase 5 of the Coupled Model Intercomparison Project (CMIP5) in terms of SM-ET coupling and showed that these uncertainties impact future warming projections. Dirmeyer et al. (2018) also suggest that models generally overestimate the control of SM on land-atmosphere fluxes, based on comparisons to available observations at flux tower sites. Despite these uncertainties, it is worth noting that studies based on model projections of future climate appear to show a general shift toward greater control of SM on ET in the future (Berg et al., 2015; Dirmeyer et al., 2012, 2013; Seneviratne et al., 2006). Such projections may be viewed as generally consistent with projections of widespread increase in future drought and aridity, and thus SM limitation, in a warmer world (Cook et al., 2014; Huang et al., 2016; Zhao & Dai, 2015).

In the present study, in order to better understand SM-ET coupling in climate models, we investigate in detail across CMIP5 models how the relationship between SM and ET manifests itself across the different components of ET. Indeed, while ET is generally treated as a single variable in climate model studies, it consists of the combination of several components: soil evaporation, plant transpiration, and canopy interception (other more minor terms include evaporation from snow and evaporation from open water on land such as lakes and rivers). The total flux, ET, is usually represented in land surface models as the sum of these three main terms, calculated separately (Lawrence et al., 2007). These three components result from different processes and thus can be expected to respond differently to physical and environmental drivers. Furthermore, because ET partitioning remains poorly constrained from observations or theory, models display large differences in the respective importance of each component (Lian et al., 2018). Several questions thus arise regarding the link between SM-ET coupling and ET partitioning in climate models: How is each component of ET linked with SM? Where are model uncertainties greatest? Does ET partitioning affect SM-ET coupling? How does SM-ET coupling evolve in future climate for each component? In this study, we address these questions, focusing on CMIP5 simulations of present and future climate and using the same diagnostics of SM-ET coupling as Berg and Sheffield (2018a).

2. Data and Methods

2.1. Data

We use monthly outputs from historical simulations and representative concentration pathway 8.5 simulations (RCP8.5; Riahi et al., 2011) from the CMIP5 experiment. We choose the RCP8.5 simulations to maximize the projected changes in the future and the potential differences between models. Our analysis primarily focuses on the following variables: total ET and its components—transpiration, soil evaporation, and canopy interception—and surface (top 10 cm) SM (variable mrsos in the CMIP5 archive). We use surface SM because it is more easily comparable across models, when correlated with surface fluxes, than total (column integrated) SM, which reflects differences in soil depths between models (e.g., Berg et al., 2017). Data for the historical simulations are analyzed over 1950–2005 and for RCP8.5 over 2071–2100. For models for which several ensemble members are available, we only use the first member ("r1" in the CMIP5 archive). We also include in our analysis and discussion a number of other variables, such as precipitation (P), Leaf Area Index (LAI), total-column SM, and the Aridity Index P/PET, where PET is Penman-Monteith potential ET (calculated from near-surface atmospheric outputs; e.g., Scheff & Frierson, 2014)

ET outputs from the historical simulations are available from 48 CMIP5 models. However, not all models provide all three variables of ET partitioning, either because of omissions or because these variables are simply not provided by the models themselves or because of errors in the reporting (e.g., the sum of two components was reported under one variable). Where possible, we correct outputs to account for obvious errors in reporting (e.g., one variable is subtracted from the sum of the other two in the other file). In addition, surface

SM is not reported for all models either. Overall, complete ET partitioning and SM together are available for 29 models from the historical simulations and 23 models for the future scenario. The number of models available for the other variables analyzed also varies. Given the limited number of models available and in order to maximize the robustness of the different statistics we compute, we use the maximum number of models available for the different variables and time periods, rather than a common set of models throughout our analysis (we indicate the number of models in the caption of the different figures). Table S1 in the supporting information lists the models used in our analysis for the different variables.

2.2. Methods

Following Berg and Sheffield (2018a), in order to analyze the strength of the terrestrial leg of SM-atmosphere coupling across models and its relationship with ET partitioning, we use a simple linear correlation between surface SM and ET components at the interannual time scale. We focus on summertime climate in each hemisphere, using seasonal mean values over June–August in the Northern Hemisphere and December–February in the Southern Hemisphere. As shown in Berg and Sheffield (2018a), positive correlation values indicate that, at the interannual time scale (from one summer to the next), SM variability controls ET variability. This can generally be expected to occur when SM availability is the limiting factor for ET. Conversely, negative values indicate that ET variations drive variations in SM levels, which can be expected to occur in regions where SM is plentiful and the limiting factor for ET becomes atmospheric evaporative demand. In addition, the correlation value quantifies how much of ET interannual variability is explained by SM variations (if the correlation is positive; vice versa if it is negative)—in other words, the tightness of the SM-ET relationship. When the correlation is positive, it quantifies the strength of SM control on ET—that is, SM limitation. As noted in Berg and Sheffield (2018a), while this remains a simple, first-order quantification of SM's impact on surface fluxes compared to more sophisticated and shorter time scale metrics (e.g., Gallego-Elvira et al., 2016), it has the advantage of being easily calculable across models and easily interpretable. Moreover, considering seasonal means removes issues associated with the coseasonality of SM and ET while still reflecting the overall (i.e., seasonally integrated) dependence of ET on SM throughout the whole season. As an example, Figure S1 illustrates interannual SM-ET correlations over one point in the central Great Plains over 55 years in the historical simulation for the different models analyzed. For that particular example at least, over the range of SM values in the different models, the relationship between SM and ET at the interannual time scale seems to lend itself well to a simple linear approach. Monthly correlations or regressions between SM and ET have been used in previous studies to assess SM-ET coupling (e.g., Berg & Sheffield, 2018a; Dirmeyer et al., 2009; Dirmeyer, 2011a; Dirmeyer et al., 2018; Santanello et al., 2018).

The interannual SM-ET correlation can be decomposed into correlations for the three main ET components as follows (noting SM for soil moisture, Tr for transpiration, E_{can} for canopy interception, and E_{soil} for soil evaporation; cov for covariance, cor for correlation, and σ for standard deviation):

$$
\begin{aligned}
\mathrm{cor}(SM, ET) &= \frac{\mathrm{cov}(SM, ET)}{\sigma_{SM}\cdot\sigma_{ET}} \\
&= \frac{\mathrm{cov}(SM, Tr + E_{can} + E_{soil})}{\sigma_{SM}\cdot\sigma_{ET}} \\
&= \frac{\mathrm{cov}(SM, Tr) + \mathrm{cov}(SM, E_{can}) + \mathrm{cov}(SM, E_{soil})}{\sigma_{SM}\cdot\sigma_{ET}} \\
&= \frac{\mathrm{cov}(SM, Tr)}{\sigma_{SM}\cdot\sigma_{Tr}}\times\frac{\sigma_{Tr}}{\sigma_{ET}} + \frac{\mathrm{cov}(SM, E_{can})}{\sigma_{SM}\cdot\sigma_{E_{can}}}\times\frac{\sigma_{E_{can}}}{\sigma_{ET}} + \frac{\mathrm{cov}(SM, E_{soil})}{\sigma_{SM}\cdot\sigma_{E_{soil}}}\times\frac{\sigma_{E_{soil}}}{\sigma_{ET}} \\
\mathrm{cor}(SM, ET) &= \mathrm{cor}(SM, Tr)\frac{\sigma_{Tr}}{\sigma_{ET}} + \mathrm{cor}(SM, E_{can})\frac{\sigma_{E_{can}}}{\sigma_{ET}} + \mathrm{cor}(SM, E_{soil})\frac{\sigma_{E_{soil}}}{\sigma_{ET}}
\end{aligned}
\tag{1}
$$

In other words, the interannual correlation between SM and ET is the sum of the interannual correlations of the three ET components with SM, weighted by the ratio of each component's (interannual) variability to (interannual) ET variability. We use this decomposition to analyze the role of individual ET components in SM-ET coupling: We calculate each term of equation (1) with outputs from CMIP5 historical and future simulations.

10.1029/2018JD029807

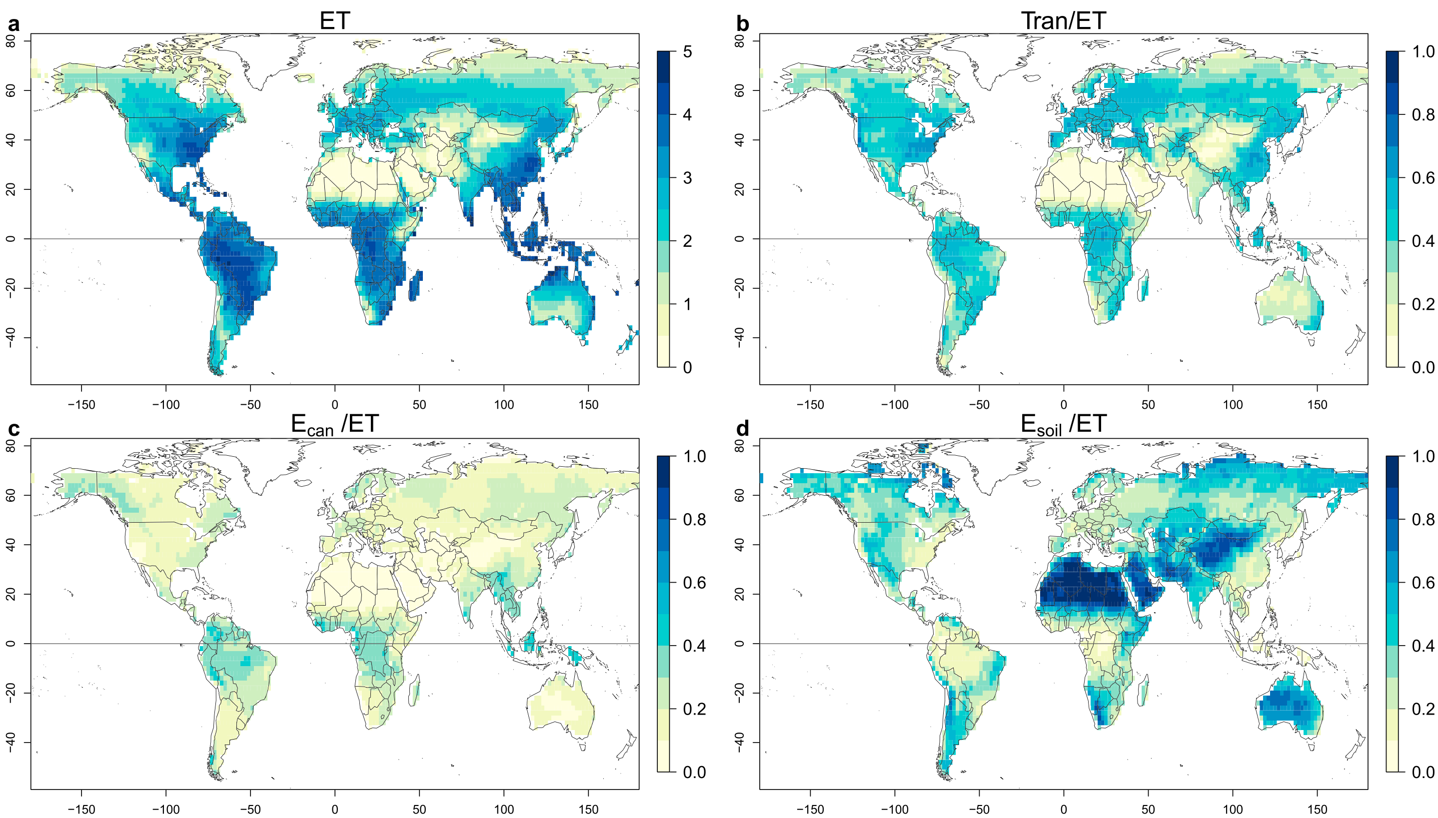

Figure 1. Multimodel mean summertime-mean values over 1950–2005 of (a) ET (mm/day) and (b–d) fractions of transpiration (Tran), canopy interception (E_{can}), and soil evaporation (E_{soil}), respectively, in total ET. Summer is defined as June-July-August in the Northern Hemisphere and December-January-February in the Southern Hemisphere. Thirty-two models with full ET partitioning are used. ET = evapotranspiration.

3. Results

3.1. Mean Summertime ET Partitioning

First, Figure 1 shows the mean summertime ET and its partitioning (results for annual means are shown on Figure S2; Figure S3 shows summertime ET partitioning in absolute values, in millimeters per day). Broadly, ET is highest in the humid Tropics and lowest in the dry subtropics and shows a secondary maximum in the midlatitudes (in the Northern Hemisphere). Because summer is generally the peak activity season for vegetation, transpiration represents the largest share of ET in many regions (up to 60% along the Equator and in the northern midlatitudes), and as a result, the spatial pattern of ET largely follows that of simulated vegetation (Figure S4). However, the fraction of transpiration tends to saturate with vegetation; as a result, even if vegetation is the densest in the Tropics, the share of transpiration is not much greater than in the midlatitudes. This is associated with a greater role played by canopy interception. Indeed, precipitation rates and LAI values are typically the two drivers of canopy interception parameterization in climate models. In the Tropics, with high rainfall and high LAI, canopy interception often amounts to 40% or more of total ET. Canopy interception also represents a large fraction of ET in some high-latitude forested regions like Alaska/Western Canada or Scandinavia, even though total LAI is lower than in the Tropics, likely because these are climatic regions where rainfall is dominated by long-duration synoptic events (Miralles et al., 2010). Finally, soil evaporation is the dominant term in dry subtropical regions with little vegetation, such as Australia, Southern Africa, or Western North America, reaching up to 60% of total ET there and up to 100% in desert regions like the Sahara and the Middle East. Note that total ET is low in these regions (Figure 1a), and in absolute terms, soil evaporation values are low as well (Figure S3). The fraction of soil evaporation still represents around 10% of ET in the Tropics; it becomes the dominant term again toward the high to very high latitudes, as vegetation decreases. Overall, on average across CMIP5 models, transpiration, soil evaporation, and canopy interception represent 43%, 33%, and 24% of mean summertime ET, respectively.

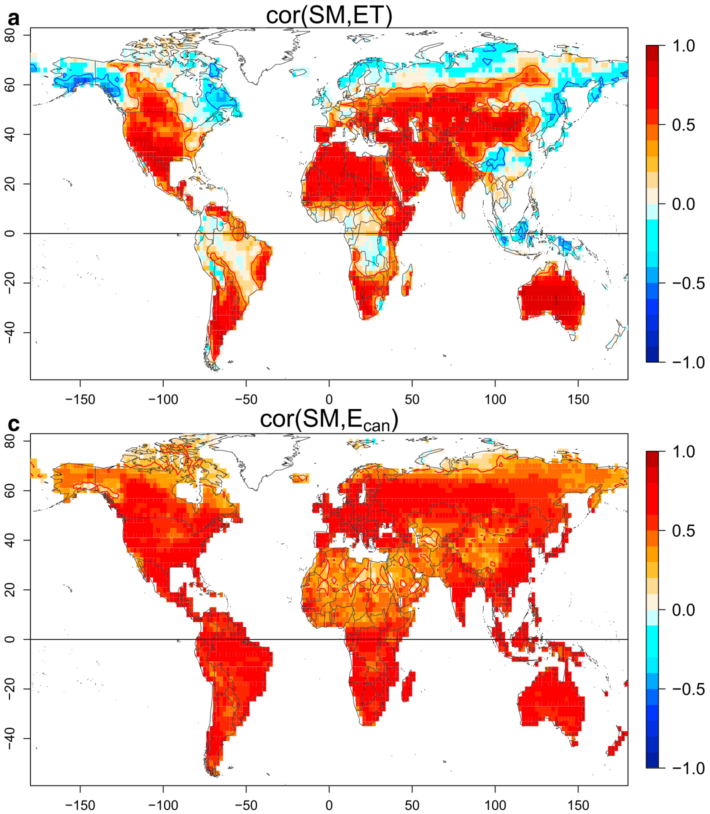

Figure 2. Multimodel mean correlation over 1950–2005 between summertime-mean surface soil moisture and (a) ET and (b) transpiration, (c) canopy interception, and (d) soil evaporation. Red and blue contour lines indicate positive and negative correlations significant at the 5% level. Twenty-nine models with full ET partitioning and soil moisture available are used. SM = soil moisture; ET = evapotranspiration.

3.2. Correlation of ET Components With SM

Figure 2a shows the mean SM-ET coupling as defined in equation (1), that is, the interannual correlation between summertime-mean surface SM and ET over the historical period (1950–2005). Correlations are positive in the subtropics and midlatitudes. These are drier regions, where ET is SM limited; consequently, ET variations are controlled by variations in SM availability. In other words, a significant share of ET variance is explained by SM variability. Conversely, negative values indicate regions where ET variations tend to drive SM variations. These are wetter regions, at high latitudes and in the tropics, where SM availability is no longer limiting for ET; ET variability is then typically driven by atmospheric evaporative demand, mostly relative to incoming solar radiation (in the Tropics) and temperature (at high latitudes; Berg & Sheffield, 2018a, 2018ab).

Figures 2b–2d show the coupling of each ET component with SM. The three main ET partitioning terms are differently coupled with SM. Both transpiration and soil evaporation show an overall coupling pattern similar to that of total ET; however, transpiration appears consistently less strongly coupled with SM (i.e., more negatively) than soil evaporation. This reflects the different parameterizations of soil evaporation and transpiration in climate models and their different sensitivities to SM availability: Our interpretation is that model transpiration is generally less constrained by SM than soil evaporation because as SM progressively decreases, vegetation in the models remains more efficient at moving water from the soil to the atmosphere than diffusion processes in the bare soil. It is worth noting that the lower coupling of transpiration is not simply a reflection of plants not depending on surface SM because of access to deeper soil: Figure S5 shows that SM-transpiration coupling is similarly low when defined using total column soil water (the coupling of soil evaporation with column soil water, on the other hand, is lower than with surface SM because soil evaporation does not physically access column soil water).

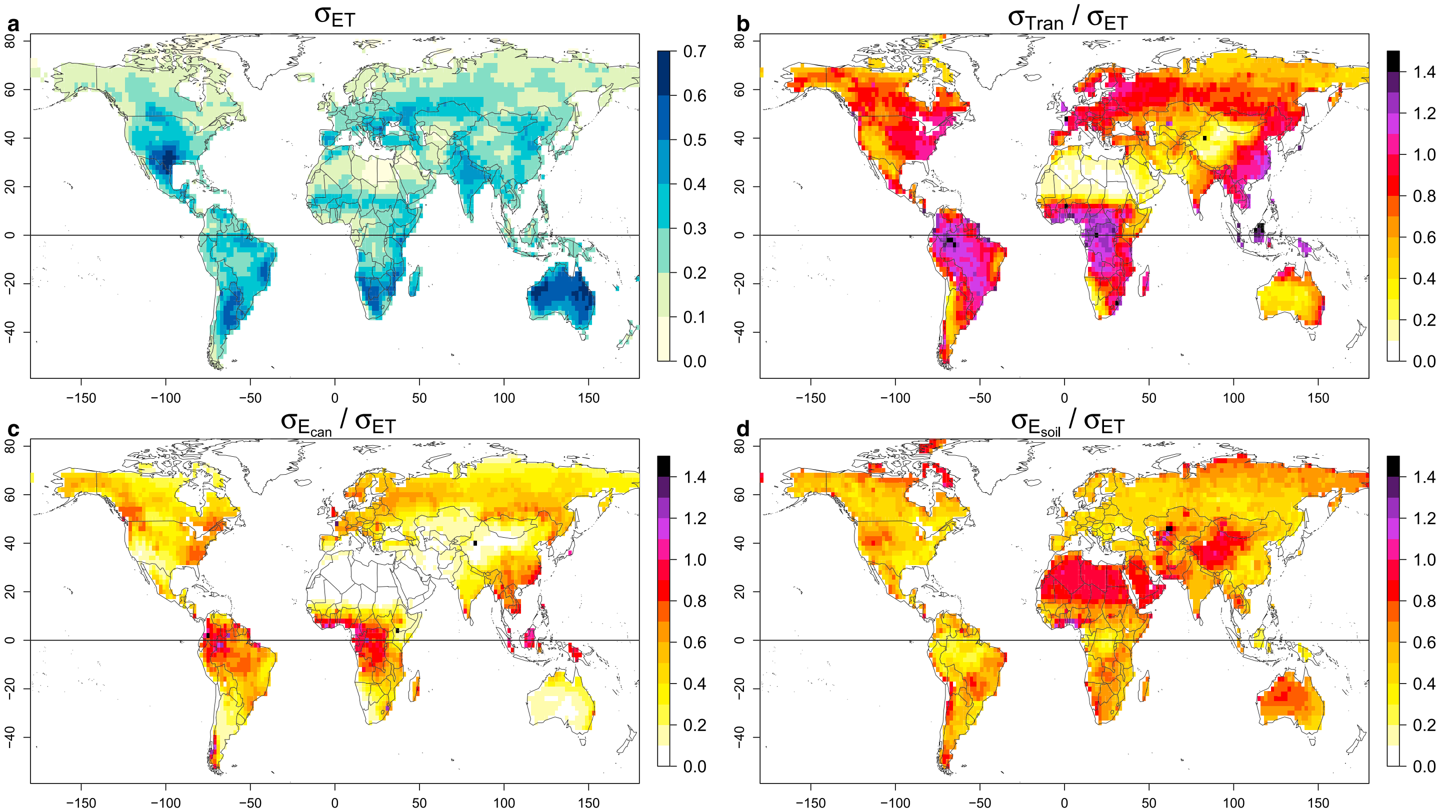

Figure 3. (a) Multimodel mean interannual standard deviation of summertime-mean ET over 1950–2005 (mm/day); (b–d) ratios of the multimodel mean interannual standard deviation of summertime-mean transpiration, canopy interception, and soil evaporation, respectively, over that of total ET, over 1950–2005. Twenty-nine models with full ET partitioning and soil moisture available are used. ET = evapotranspiration.

Figure 2c shows that canopy interception is always positively coupled with SM, including in regions where total SM-ET coupling is nil or negative (in the multimodel mean). This reflects the fact that canopy interception happens during rainfall events, during which SM also increases. Therefore, canopy interception and SM appear positively correlated; however, this correlation is noncausal, as it does not reflect any actual physical process by which SM constrains canopy interception. Rather, it is a correlation forced by precipitation occurrence. It is noteworthy that in the Tropics and high latitudes, this positive correlation is opposite to that of transpiration: In such regions, while greater canopy interception takes place with higher rainfall, transpiration is driven by atmospheric evaporative demand, which is greater in the absence of rainfall (i.e., with increased solar radiation and higher temperature). Figure S5 shows that the coupling of canopy interception with column soil water is lower than with surface SM, reflecting the fact that column SM is not as strongly linked with precipitation as surface SM, so that the apparent correlation with canopy interception (which, itself, depends on precipitation) is weaker.

3.3. Decomposing SM-ET Coupling Within ET Components

As indicated in equation (1), the correlation between SM and ET is equal to the sum of the correlations of the three ET components with SM, weighted by the ratio of each component's (interannual) variability to (interannual) ET variability. Here we analyze these weights and the corresponding full terms of SM-ET coupling that can be attributed to each ET component (i.e., the product of the correlation to SM and the standard deviation ratio).

Interannual variability of summertime-mean ET is greatest in regions of greatest interannual precipitation variability, such as monsoon regions (Sahel, India, and Australia), as well as some midlatitude regions (Figure 3a). Figures 3b–3d show that the mean ratios of the variability of each ET component to the variability of total ET largely follow the mean ET partitioning shown on Figure 1. However, there is not a one-

10.1029/2018JD029807

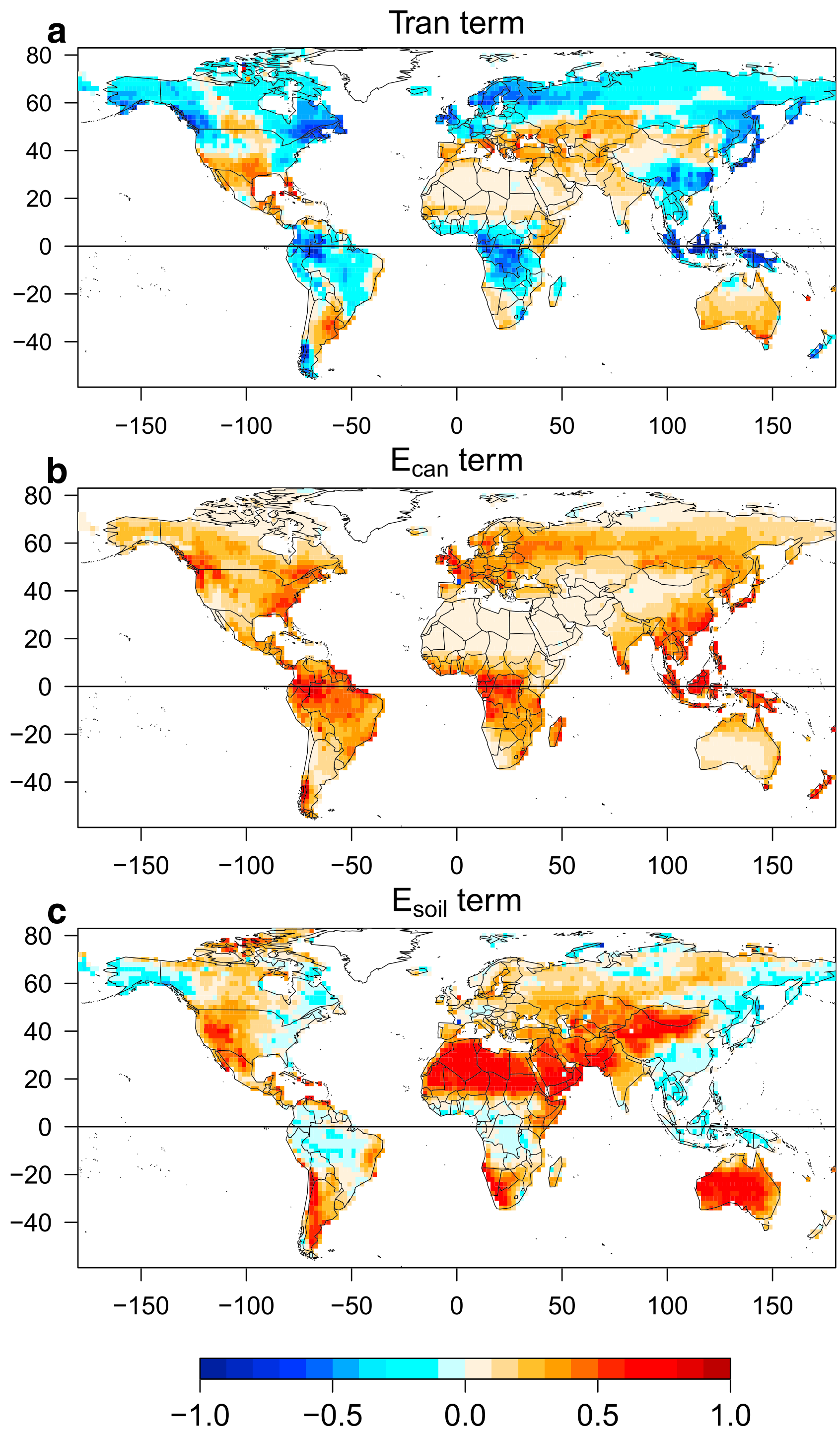

Figure 4. (a–c) Multimodel mean components of soil moisture-evapotranspiration coupling, according to equation (1) attributable to transpiration, canopy interception, and soil evaporation, respectively.

to-one relationship across models between both terms (not shown), indicating that the relationship between the mean value and the variability of each ET component is not necessarily the same for each model. Note that the standard deviation ratios can be greater than one, to the extent that the different ET components vary in opposite ways; that is, a particular summer with more transpiration will have less soil evaporation (in relative terms but also in absolute terms; Figure S6).

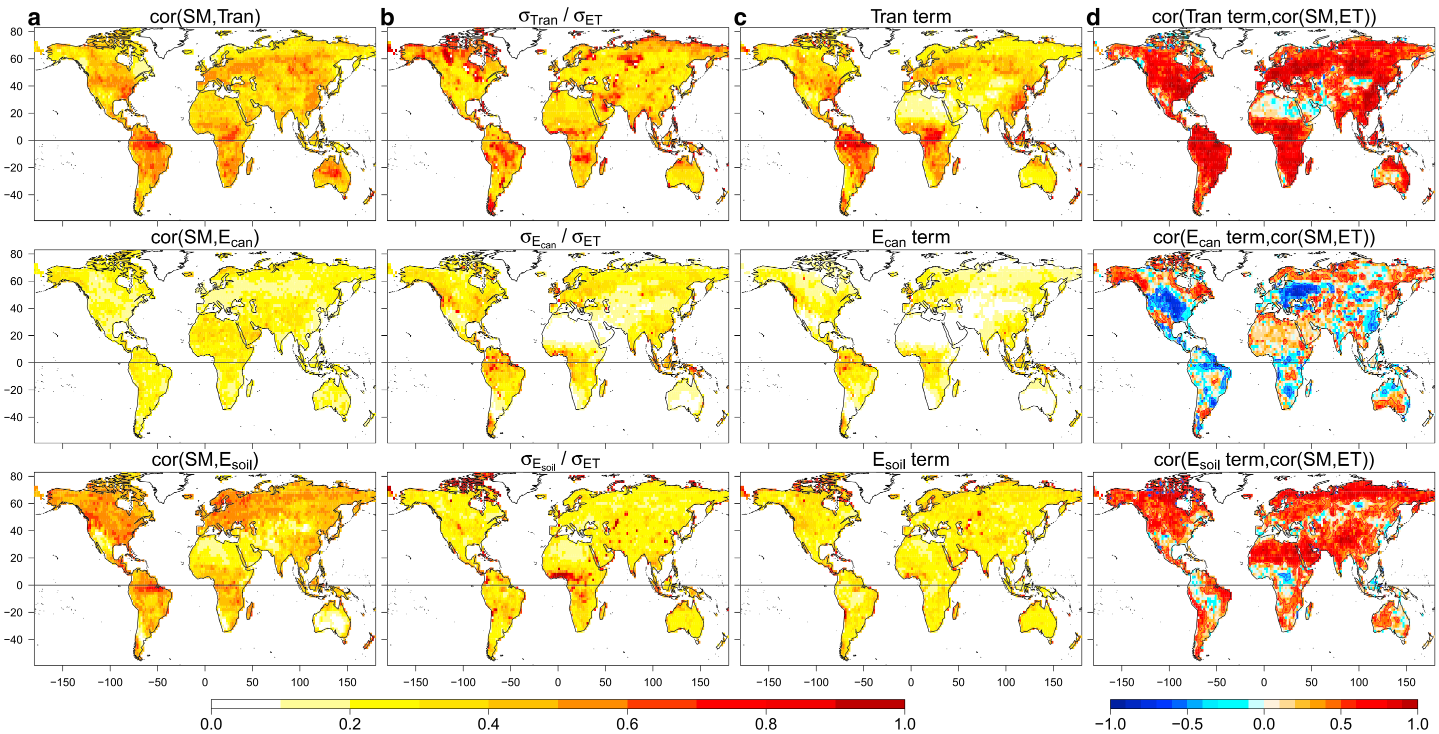

Figure 5. Cross-model standard deviation of (a) the correlation over 1950–2005 of ET components with soil moisture; (b) the ratio of interannual variability of ET components to ET variability; (c) the full component of SM-ET coupling attributable to each ET component, for (from top to bottom) transpiration, soil evaporation, and canopy interception. (d) Cross-model correlation between the components of SM-ET coupling attributable to each ET term and total SM-ET coupling; red and blue contour lines indicate positive and negative correlations significant at the 5% level; 29 models with full ET partitioning and soil moisture available are used. SM = soil moisture; ET = evapotranspiration.

Figure 4 then shows the total terms of SM-ET coupling that can be attributed to each ET component. Comparison of Figures 2a and 4 shows that the positive coupling of SM and ET, overall, mostly arises from the contribution of soil evaporation (Figure 4c) in dry regions (subtropics), with lesser contribution from transpiration in the same regions. Indeed, because transpiration represents a lower share of total ET and total ET variability in dry regions (Figure 3b), the positive correlation of transpiration with SM, which was already low (Figure 2b), contributes even less to the overall positive SM-ET correlations in those regions (Figure 4a). In wetter regions, such as the Tropics and high latitudes, the negative correlation between transpiration and SM is magnified by the large role of transpiration in ET variability, resulting in a large negative contribution. Thus, globally, the contribution of transpiration to SM-ET coupling actually appears mostly negative. However, the negative contribution of transpiration in the Tropics and high latitudes is masked by the positive contribution from canopy interception. Indeed, canopy interception contributes positively to SM-ET coupling in those regions, as the correlation with SM is positive everywhere (Figure 2c) and canopy interception represents a substantial part of (interannual) ET variability in those regions (Figure 3c). This positive contribution (Figure 4b) almost completely overlaps with the negative transpiration term (Figure 4a). As a result, the overall SM-ET coupling in these regions remains close to zero (Figure 2a). The contribution of canopy interception in drier, subtropical regions (where soil evaporation and transpiration contributes positively and total SM-ET coupling is positive) is close to zero, reflecting the almost nil contribution of canopy interception to ET variability in those regions (Figure 3c). Only on the outer margins of those regions does the positive canopy interception term overlap with positive contributions from soil evaporation and transpiration and contributes to positive SM-ET coupling. Overall, Figure 4 shows that SM-ET coupling is the result of very different contributions from the different components of ET.

3.4. Uncertainties in SM-ET Coupling and ET Components

We now focus on the multimodel spread in SM-ET coupling and how it relates to the contributions from the different ET components. The multimodel spread in total SM-ET coupling was discussed in Berg and

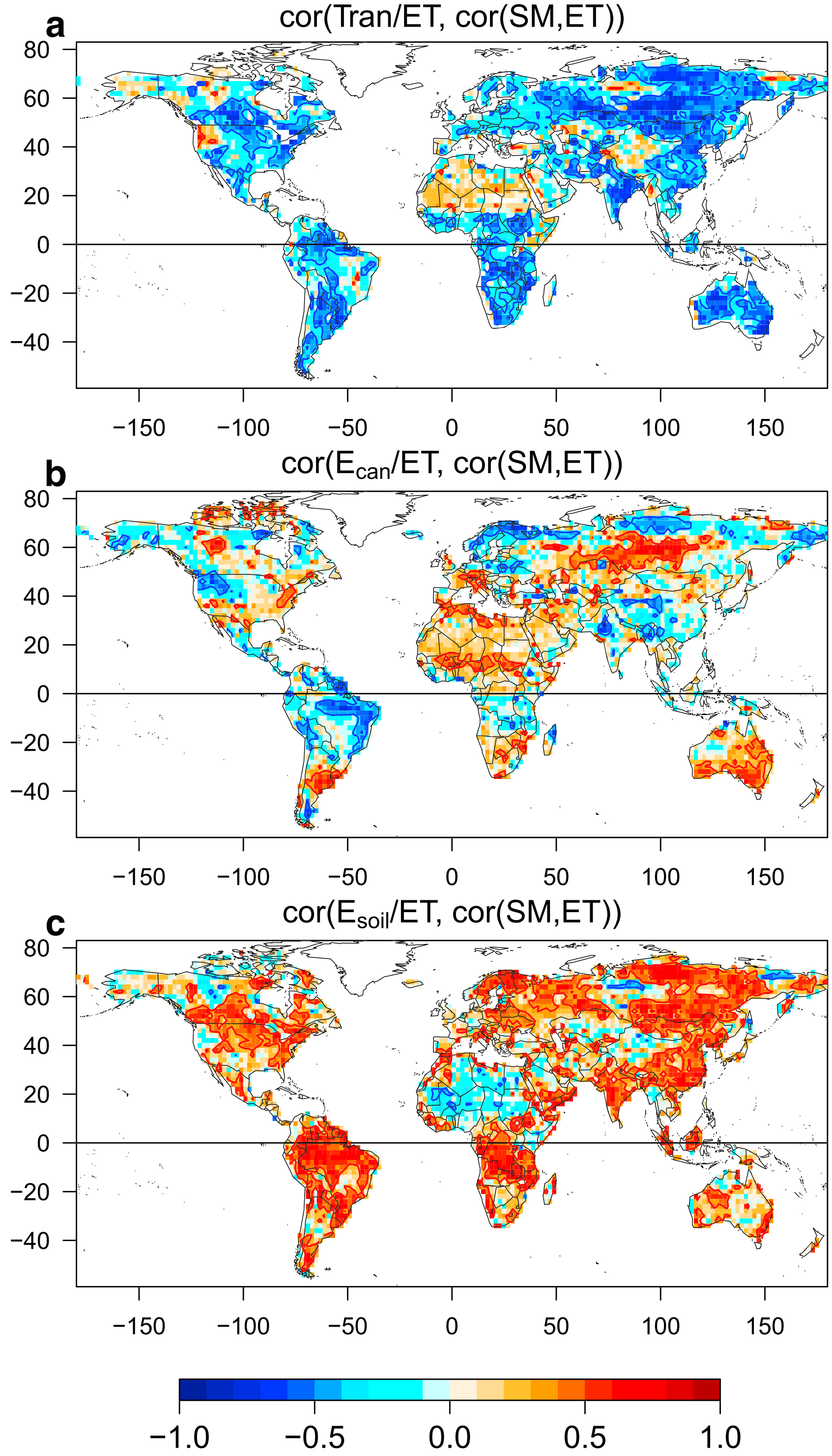

Figure 6. Cross-model correlation between historical (1950–2005) SM-ET coupling and mean fraction of (a) transpiration, (b) soil evaporation, and (c) canopy interception in total summertime ET. Red and blue contour lines indicate positive and negative correlations significant at the 5% level. Twenty-nine models with full ET partitioning and soil moisture available are used. SM = soil moisture; ET = evapotranspiration.

Sheffield (2018a) and is shown on Figure S7. Figure 5a shows that the multimodel spread in coupling with SM, as characterized by the cross-model standard deviation, is generally largest for transpiration and soil evaporation. However, in regions where soil evaporation represents a larger share of total ET

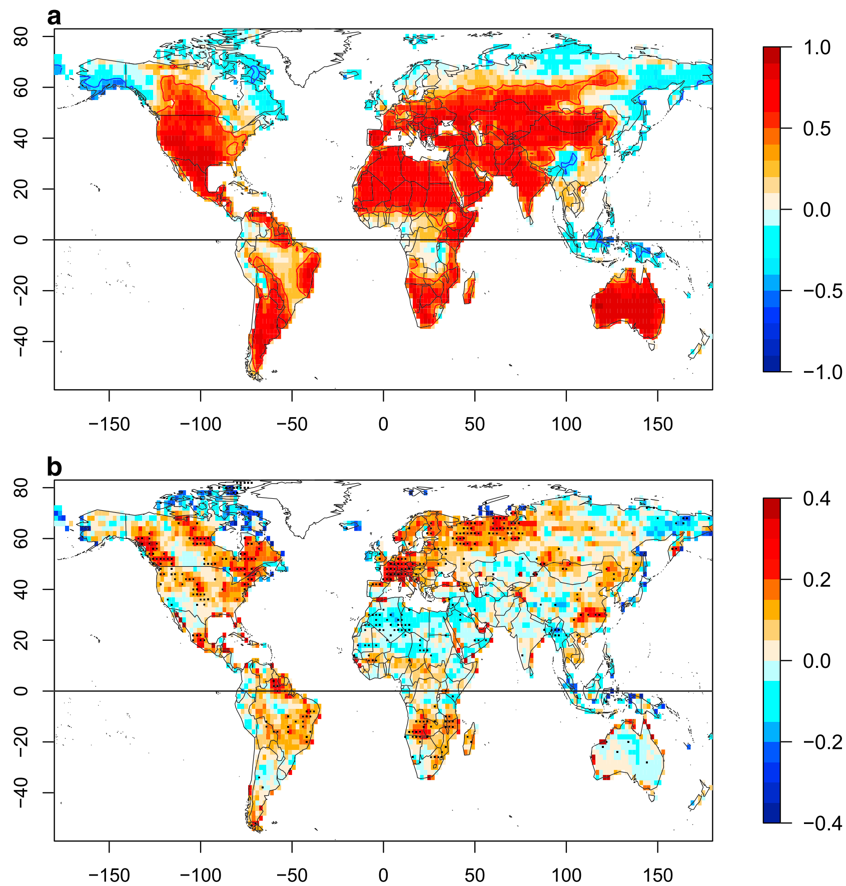

Figure 7. (a) Multimodel mean correlation between summertime-mean surface soil moisture and evapotranspiration over 2071–2100; red and blue contour lines indicate positive and negative correlations significant at the 5% level. (b) Multimodel mean change from 1950–2005 (note the different scale from (a)). Stippling indicates where more than three quarters of the models agree on the sign of the projected changes. Twenty-three models with full evapotranspiration partitioning and soil moisture available in the future (and present) scenarios are used.

(Figure 1), model spread is actually low. In contrast, SM-transpiration coupling shows large model uncertainties including in tropical and midlatitudes regions where transpiration represents a large share of total ET. One interpretation is that this reflects the fact that those are wetter regions, which might be closer to the threshold for SM limitation and thus where models may be more likely to disagree on whether transpiration should be SM-limited, in particular depending on model differences in regional precipitation. In contrast, models are more likely to agree on SM strongly limiting water fluxes in dry regions where soil evaporation dominates. However, even in dry regions, SM-transpiration coupling shows more model uncertainties than SM-soil evaporation coupling. This suggests that the coupling of transpiration with SM is more uncertain, across models, than that of soil evaporation. By comparison, there appears to be little uncertainty across models in the correlation between SM and canopy interception. This suggests that the parameterization of canopy interception is largely similar across models, at least in terms of its sensitivity to precipitation (and thus its apparent sensitivity to SM).

The model spread in the standard deviation ratios is also generally larger for transpiration than for the other terms (Figure 5b). As a result, model spread in the total component of SM-ET coupling attributable to each partitioning term is clearly greatest for transpiration (Figure 5c). In particular, model spread remains low for the soil evaporation term despite the large uncertainty in SM-soil evaporation coupling in many regions, because in these regions, soil evaporation actually represents only a small share of ET variability on average. The model spread for the canopy interception term (Figure 5c) also remains low, given the agreement between models in terms of the SM-canopy interception correlation (Figure 5a).

10.1029/2018JD029807

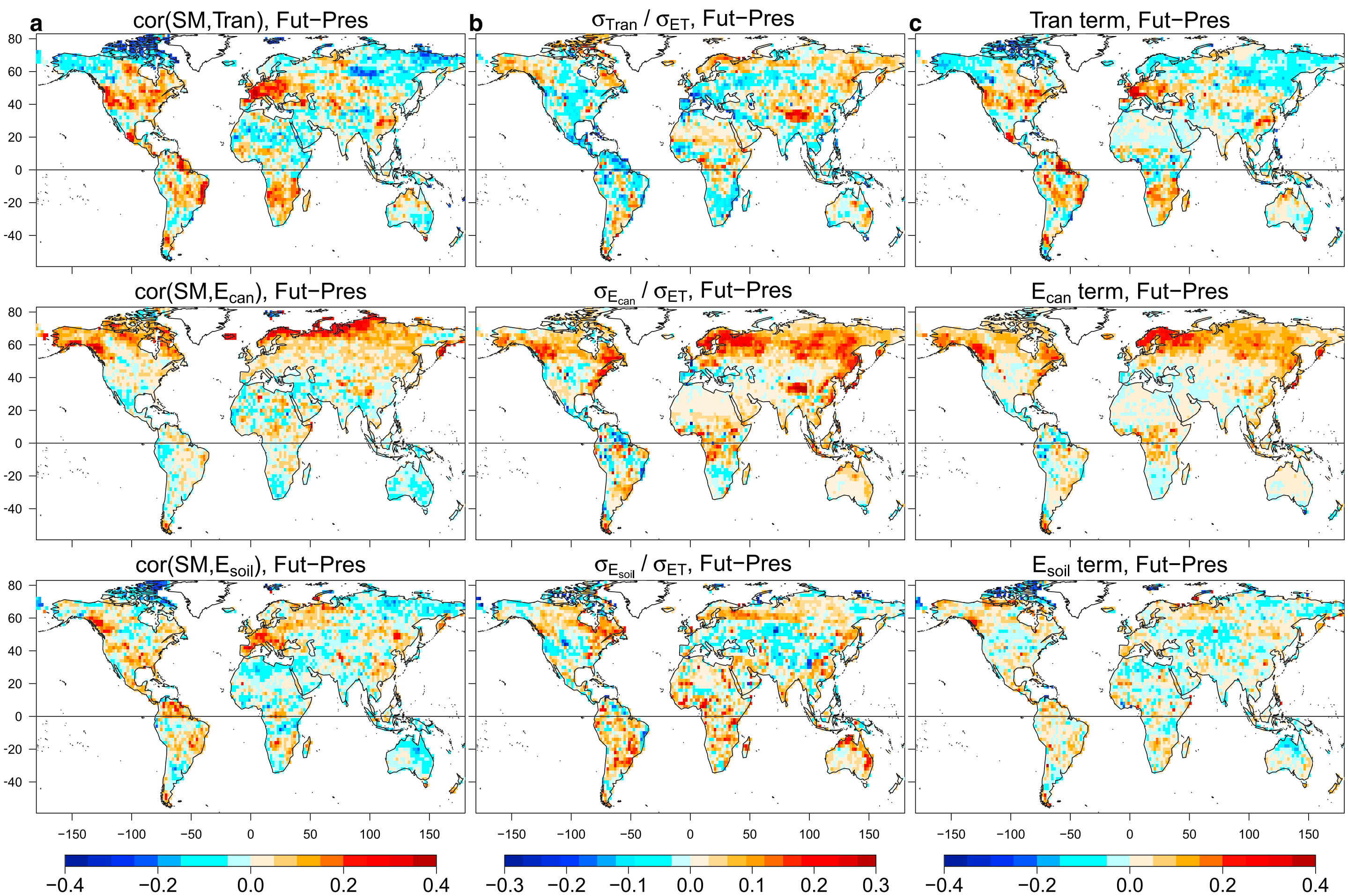

Figure 8. Multimodel mean change, from 1950–2005 to 2071–2100, in (a) the correlation of each ET component with soil moisture; (b) the ratio of interannual variability of each ET component to ET variability; (c) the full component of SM-ET coupling attributable to each ET component, for (from top to bottom) transpiration, soil evaporation, and canopy interception. Note the difference in scale between (a), (b), and c). Twenty-three models with full ET partitioning and soil moisture available in the future (and present) scenarios are used. SM = soil moisture; ET = evapotranspiration.

Model differences in the transpiration component of SM-ET coupling explain most of the variance across models in total SM-ET coupling (Figure 5d). Model differences in the soil evaporation component of coupling only significantly explain uncertainties in SM-ET coupling in dry, desert-type regions (where model spread is lowest in the first place; Figure S7), as well as in high latitude regions where soil evaporation is the dominant term in ET and ET variability (Figures 1 and 3). For both transpiration and soil evaporation, this contribution mostly comes from the model spread in coupling with SM rather than the spread in the standard deviation ratios (not shown). Finally, the model spread in the canopy interception component of SM-ET coupling, which is low (Figure 5c), explains little of the spread in SM-ET coupling; actually, the canopy interception term tends to be negatively correlated with SM-ET coupling across models, in particular in some midlatitude regions (Eastern Europe and USA). This might seem surprising given that both quantities are, on average across models, positive over these regions (Figures 2a and 4c). However, this mostly reflects an underlying relationship with transpiration: In these regions, the contributions of canopy interception and transpiration to SM-ET tend to be anticorrelated across models (not shown). This likely reflects the common role of model differences in precipitation in forcing both aspects (higher precipitation reducing SM control on transpiration and enhancing the role of canopy interception). Thus, because of the dominant role of transpiration in explaining model spread in SM-ET coupling, the canopy interception term appears negatively correlated with overall SM-ET coupling in these regions (Figure 5d).

Finally, we analyze whether mean ET partitioning affects overall SM-ET coupling. Figure 6 shows the correlation between mean ET partitioning and SM-ET coupling. In many regions, models with less

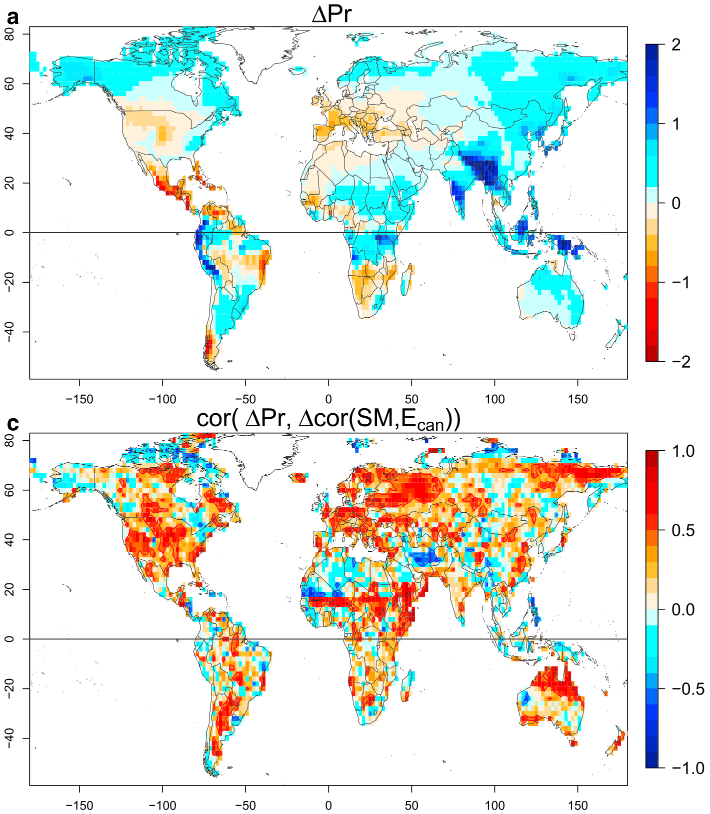

Figure 9. (a) Multimodel mean change in summertime-mean precipitation between 1950–2005 and 2071–2100 (mm/day); (b–d) correlation across models between summertime change in precipitation and change in the contribution to SM-evapotranspiration coupling of transpiration, canopy interception, and soil evaporation, respectively. Twenty-three models with full evapotranspiration partitioning and soil moisture available in the future (and present) scenarios are used. SM = soil moisture.

transpiration and/or more soil evaporation tend to show greater coupling of ET with SM. This may partly reflect the fact that models with greater precipitation are more likely to both be less SM-limited and show greater transpiration fractions; however, this is also consistent with the different coupling values for each component (Figure 2), that is, that transpiration is less positively coupled with SM than soil evaporation. Models that favor transpiration will thus exhibit weaker SM-ET coupling. This cross-models relationship, across the CMIP5 ensemble, is also consistent with the changes in simulated land-atmosphere coupling and surface climate characteristics reported in previous studies in which ET partitioning was deliberately altered in a given model (Lawrence et al., 2007; Williams et al., 2016).

3.5. Changes in SM-ET Coupling and Its Components in Future Projections

We now turn to changes in SM-ET coupling in future climate projections. Figure 7 shows that globally, SM-ET coupling becomes more positive, with increases in parts of the Tropics and in many regions of the northern mid-to-high latitudes: Northern United States and Canada, Central Europe, Northern Europe and Russia, and Eastern China. No large regions display substantial decrease in SM-ET coupling. Thus, Figure 7 indicates that in future projections, ET generally appears to become more strongly controlled by SM availability. A large part of that increase corresponds to a northward extension (in the northern hemisphere) of the area of positive summertime SM-ET coupling. This is consistent with previous studies showing a general shift toward greater control of SM on ET in climate model projections of future climate (Berg et al., 2015; Dirmeyer et al., 2012, 2013; Seneviratne et al., 2006).

Figures 8a and 8b show the decomposition of the overall change in SM-ET coupling into its different components: changes in the correlations between SM and ET components and in the standard deviation ratios, of each term to total ET; Figure 8c shows changes in the overall coupling term for each component. Consistent with Figure 7, all three components of ET show, overall, a more positive correlation with SM

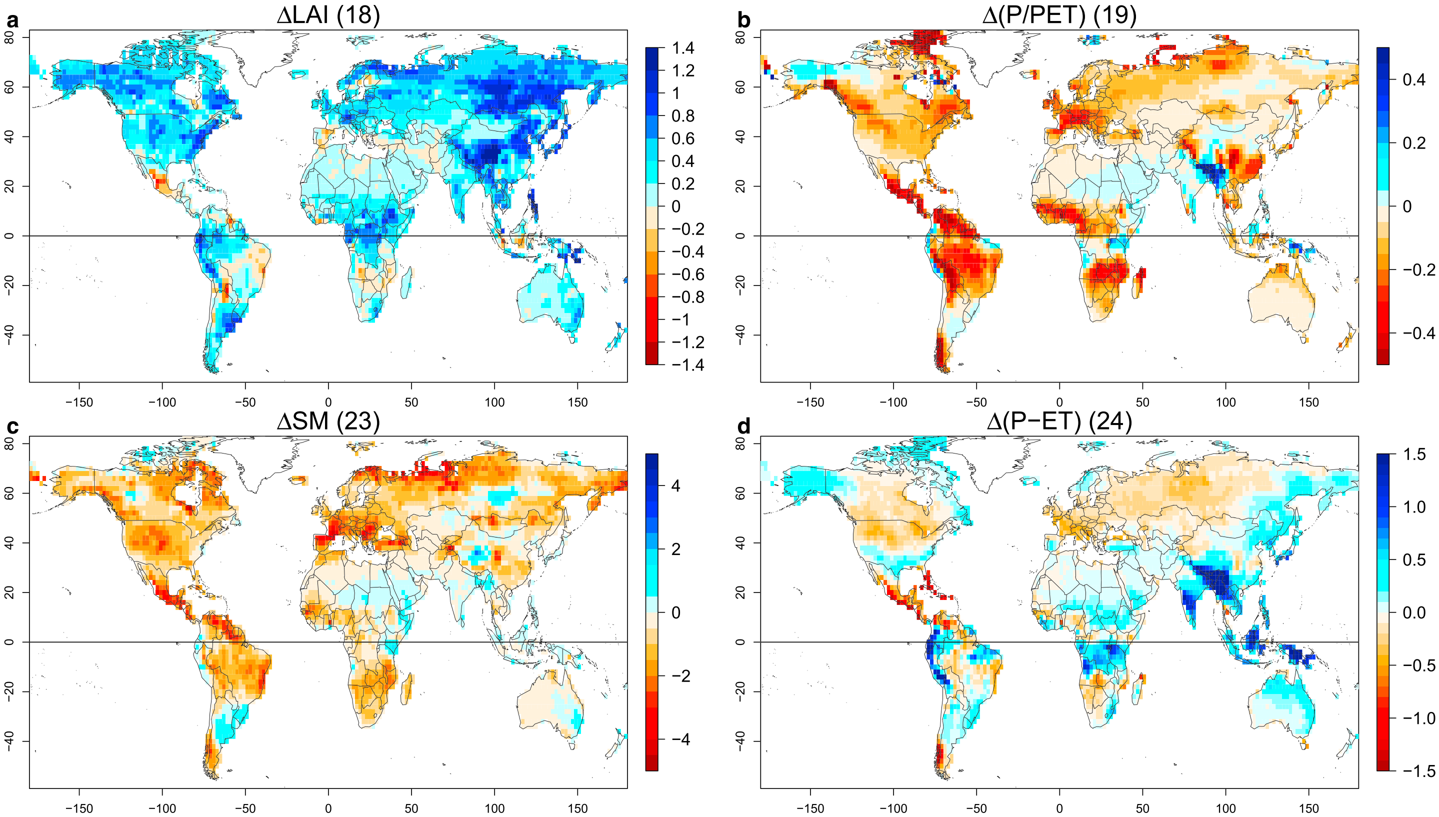

Figure 10. Multimodel mean projected changes between 1950–2005 and 2071–2100 in summertime-mean (a) LAI (–), (b) P/PET (–), (c) surface soil moisture (mm), and (d) P-ET (mm/day). The numbers in parentheses indicate the number of models used in each panel plot, which is determined as the number of models for which both changes in future ET partitioning and in the variable plotted were available. LAI = Leaf Area Index; precipitation; PET = Penman-Monteith potential ET; SM = soil moisture; ET = evapotranspiration.

in the future, with large regions with slight (positive or negative) changes and a few regions of stronger increase (Figure 8a). The increase in coupling for transpiration takes place in the same overall regions as SM-ET coupling, except for the high latitudes. Soil evaporation behaves essentially like transpiration, with more modest increases, in particular in the Tropics. In contrast, canopy interception shows a different pattern, becoming more positively correlated with SM predominantly at high latitudes. Further, Figure 8b shows that the predominant change in terms of standard deviation ratios is that the variability of canopy interception as a fraction of the variability of total ET increases, in particular in the northern mid-to-high latitudes (north of 50°N). In contrast, the ratio of transpiration variability to total ET variability slightly decreases in many regions. As a result, while transpiration is the dominant term in the overall SM-ET coupling increase in the Tropics and midlatitudes regions (e.g., Europe and USA; Figure 8c), the increase in the contribution from canopy interception explains most of the increase in SM-ET coupling at higher latitudes (e.g., north of 50°N). The contribution of soil evaporation to coupling changes remains very limited, because the increases in SM-soil evaporation correlations occur in regions where soil evaporation represents a small fraction of total ET.

The increase in the contribution of transpiration to SM-ET coupling is consistent with increased SM control in regions where summertime precipitation is projected to decrease (Figure 9a) and in regions where transpiration dominates the partitioning of ET (Figure 1). The increase in the contribution of canopy interception, on the other hand, is consistent with a projected increase in both vegetation (Figure 10a) and precipitation at higher latitudes (Figure 9a). These increases reinforce the noncausal, rainfall-forced correlation between SM and canopy interception and also increase how much of the interannual variability of ET is caused by canopy interception. Consistent with the above, Figures 9b–9d show that while changes in the contribution from transpiration and soil evaporation are both negatively correlated across models with changes in precipitation (as more precipitation reduces SM limitation), the contribution of canopy interception is positively correlated with it: Models where rainfall increases more see a greater increase in the contribution from canopy interception to SM-ET coupling. Thus, at high latitudes, the increase in overall SM-ET coupling does not reflect increased direct SM limitation on ET, as could be suggested by the increase in overall SM-ET coupling; rather, it reflects the increased importance of canopy interception in ET variability and its relationship with precipitation, as vegetation increases.

4. Discussion and Conclusion

The control of SM availability on ET is a critical process in land-atmosphere interactions and climate as well as for the terrestrial water cycle. Here, for the first time, we have investigated how the relationship between SM and ET emerges from the different components of ET in current-generation climate models, both in historical and future simulations.

We have shown that the individual components of ET are differently coupled with SM (Figure 2). On average, transpiration and soil evaporation share the same spatial pattern of coupling with SM, but transpiration is much less strongly coupled: Positive correlations indicating SM control are lower than for soil evaporation, and in many parts of the Tropics and high latitudes, correlations are negative, as energy-driven ET variations drive variations in SM. This difference indicates that vegetation processes in models are more efficient at extracting water from the soil to the atmosphere than soil diffusion processes involved in soil evaporation. Thus, transpiration appears more energy-limited and less SM limited than soil evaporation. In contrast to soil evaporation and transpiration, canopy interception is systematically positively correlated with SM; however, this correlation is noncausal and reflects the indirect role of precipitation in forcing both variables, rather than an actual physical constraint of SM on canopy interception.

Decomposing SM-ET coupling into terms attributable to each ET component (by accounting for the share of each component in ET variability; Figure 3) shows that the contribution of transpiration is mostly negative, with soil evaporation being the dominant positive term (Figure 4). A sizeable part of the overall SM-ET coupling actually reflects the positive contribution from the canopy interception term. Overall, the share of the three ET terms (as shown on Figure 4) in total SM-ET coupling (i.e., for each component, the global mean of the ratio of the absolute value of that term with the sum of the absolute values of the three terms) is 30%, 33%, and 37% for transpiration, canopy interception, and soil evaporation, respectively. The positive contribution from canopy interception tends to mask the negative contribution of transpiration in the Tropics and high latitudes. This shows that coupling of ET to SM is a complex response combining the different relationships of each ET component with SM (Figure 2), as well as the different role of each term in ET variability (Figure 3), which is partly linked to ET partitioning. Our results also show that, because of the different way, each ET component is coupled with SM; model differences in mean ET partitioning affect overall SM-ET coupling (Figure 6). This is consistent with single-model studies where ET partitioning was modified (e.g., Lawrence et al., 2007). In particular, models that favor soil evaporation tend to be more strongly SM limited.

More generally, our results emphasize that ET may not just be simply considered in climate studies as a single-process variable and as, to some extent, the land counterpart to oceanic evaporation, but that it is really a complex variable whose components obey different, and sometimes opposite, drivers. Here the overall SM-ET coupling should be interpreted with caution when inferring how it reflects the behavior of individual ET components. In particular, canopy interception plays a confounding role, systematically skewing SM-ET coupling toward positive values. This issue is illustrated by future projections of SM-ET coupling, which show a robust, widespread correlation increase (Figure 7b). This increase may be interpreted, at first glance, as further evidence of a widespread increase in aridity and SM limitation in a warmer world, in particular in the mid-to-high latitudes (e.g., north of 50°N). Indeed, many studies, based on model projections of near-surface climate and on associated aridity or drought metrics, such as the ratio of precipitation to evaporative demand (P/PET), project a widespread increase in droughts and aridity over land, including in mid-to-high latitudes regions that show little or even positive changes in precipitation (e.g., Cook et al., 2014; Huang et al., 2016; Zhao & Dai, 2015). These projections are often interpreted as reflecting the role of warming in increasing evaporative demand and drying out the surface (e.g., Cook et al., 2014). Such projections include increased aridity over regions north of 50°N, such as eastern and western Canada and northern Europe and Asia (Figure 10b; see also, e.g., Zhao & Dai, 2015). Surface SM projections from climate models also indicate widespread decreases, including in the same northern regions, which appear consistent with projections of increased aridity (Figure 10c; see also, e.g., Berg et al., 2017). In this context, widespread increases in SM control on ET in the same regions (Figure 7b) would appear consistent, too, with these projections, indicating a more arid and more water-limited climate, even though such regions show only modest negative changes, or even positive ones, in summer precipitation (Figure 9a). However, we showed here that in these mid-to-high latitude regions (north of 50°N), the increase in SM-ET coupling mainly reflects the increased importance of canopy interception in ET variability and the increased positive relationship with precipitation, as both vegetation and precipitation are projected to increase; SM limitation on transpiration in such regions actually decreases slightly (Figure 8c). Berg et al. (2017) further showed that the negative change in summertime SM in northern latitudes (north of 50°N) is consistent with a negative change in P-ET, which itself results from a greater increase in ET than in P (Figure 10d). In our interpretation, climate model projections in these regions thus depict a continental environment in which warming and increased vegetation lead to increased ET, thus depleting SM. However, this decrease in SM does not lead to increased soil water limitation on transpiration (Figure 8c): The increased SM-ET correlation actually only reflects the increased role of canopy interception, caused by enhanced vegetation and precipitation. Aridity metrics such as P/PET, on the other hand, reflect the warming and drying (e.g., relative humidity) of the near-surface atmosphere, but these changes are not necessarily directly indicative of adverse impacts on vegetation and soil water limitation. In that sense, by focusing on individual ET components and their relationship with SM, our results help interpret concurrent model projections of future terrestrial hydrology, vegetation, and climate, which in some respects can appear conflicting in certain regions (e.g., Berg & Sheffield, 2018b, and references therein).

On the other hand, we also show that in regions of summertime precipitation decrease (south of 50°N: Western Europe and USA), SM control on transpiration does increase on average in the future (Figure 8c). This is consistent with recent results from Trugman et al. (2018), who analyzed SM stress on transpiration in detail in a subset of CMIP5 models and showed a slight increase in SM stress in future projections. Nevertheless, in models at least, vegetation in these regions is still projected to increase (Figure 10a), indicating that the increase in SM limitation does not appear severe enough to reverse the increase in vegetation induced by CO_2 fertilization and other changes in climate.

One limitation of our analysis is that it focuses on only one season (summer). Results regarding the contribution of the different ET components to SM-ET coupling may differ for other months or seasons. For instance, depending in particular on the regional seasonality of precipitation, transpiration may be more water-limited (in the models) in the spring (e.g., in regions with summer-dominated rainfall seasons) or in the late summer or fall (in regions with a springtime-dominated rainfall regime). Similarly, projections for future changes in the contribution of each ET components may differ for different seasons, depending on future seasonal changes in moisture availability. Further work will be needed to more comprehensively assess present-day and future seasonal SM control on ET components.

Finally, our results also show that transpiration exhibits the most uncertainty across models in terms of coupling with SM (Figure 5d). Thus, because of the dominant role of transpiration in total ET, model differences in SM-transpiration coupling explain most of the model spread in overall SM-ET coupling. This model spread is consistent, again, with Trugman et al. (2018), who showed large uncertainties in the simulated mean SM stress on transpiration and photosynthesis in a subset of models: Models appear to struggle to robustly represent the relationship between SM and transpiration. These results thus provide further motivation for the land modeling and observation community to improve the simulation of hydrologic stress in global vegetation and climate models, which often remains reliant on simple parameterizations based on SM levels, toward more process-based representation of soil-plant-atmosphere water dynamics.

Acknowledgments

This work was supported by NOAA grant NA15OAR4310091. We acknowledge the World Climate Research Programme's Working Group on Coupled Modelling, which is responsible for CMIP, and we thank the climate modeling groups (listed in Table S1) for producing and making available their model output. All the model data used in this study can be accessed through the Earth System Grid Federation (ESGF; e.g., https://esgf-node.llnl.gov/projects/esgf-llnl/). For CMIP, the U.S. Department of Energy's Program for Climate Model Diagnosis and Intercomparison provides coordinating support and led development of software infrastructure in partnership with the Global Organization for Earth System Science Portals.

References

Berg, A., Lintner, B. R., Findell, K., Seneviratne, S. I., van den Hurk, B., Ducharne, A., et al. (2015). Interannual coupling between summertime surface temperature and precipitation over land: Processes and implications for climate change. *Journal of Climate*, *28*(3), 1308–1328. https://doi.org/10.1175/JCLI-D-14-00324.1

Berg, A., & Sheffield, J. (2018a). Soil moisture–evapotranspiration coupling in CMIP5 models: Relationship with simulated climate and projections. *Journal of Climate*, *31*(12), 4865–4878. https://doi.org/10.1175/JCLI-D-17-0757.1

Berg, A., & Sheffield, J. (2018b). Global warming and drought: The soil moisture perspective. *Current Climate Change Reports*, *4*(2), 180–191. https://doi.org/10.1007/s40641-018-0095-0

Berg, A., Sheffield, J., & Milly, P. C. (2017). Divergent surface and total soil moisture projections under global warming. *Geophysical Research Letters*, *44*, 236–244. https://doi.org/10.1002/2016GL071921

Cook, B. I., Smerdon, J. E., Seager, R., & Coats, S. (2014). Global warming and 21st century drying. *Climate Dynamics*, *43*(9-10), 2607–2627. https://doi.org/10.1007/s00382-014-2075-y

Dirmeyer, P. A. (2011a). The terrestrial segment of soil moisture–climate coupling. *Geophysical Research Letters*, *38*, L16702. https://doi.org/10.1029/2011GL048268

Dirmeyer, P. A. (2011b). A history of the Global Soil Wetness Project (GSWP). *Journal of Hydrometeorology*, *12*(5), 729–749. https://doi.org/10.1175/JHM-D-10-05010.1

Dirmeyer, P. A. (2018). Coupled from the start. *Eos*, *99*. https://doi.org/10.1029/2018EO095367

Dirmeyer, P. A., Cash, B. A., Kinter, J. L. III, Stan, C., Jung, T., Marx, L., et al. (2012). Evidence for enhanced land–atmosphere feedback in a warming climate. *Journal of Hydrometeorology*, *13*(3), 981–995. https://doi.org/10.1175/JHM-D-11-0104.1

Dirmeyer, P. A., Chen, L., Wu, J., Shin, C. S., Huang, B., Cash, B. A., et al. (2018). Verification of land–atmosphere coupling in forecast models, reanalyses, and land surface models using flux site observations. *Journal of Hydrometeorology*, *19*(2), 375–392. https://doi.org/10.1175/JHM-D-17-0152.1

Dirmeyer, P. A., Jin, Y., Singh, B., & Yan, X. (2013). Trends in land–atmosphere interactions from CMIP5 simulations. *Journal of Hydrometeorology*, *14*(3), 829–849. https://doi.org/10.1175/JHM-D-12-0107.1

Dirmeyer, P. A., Koster, R. D., & Guo, Z. (2006). Do global models properly represent the feedback between land and atmosphere? *Journal of Hydrometeorology*, *7*(6), 1177–1198. https://doi.org/10.1175/JHM532.1

Dirmeyer, P. A., Schlosser, C. A., & Brubaker, K. L. (2009). Precipitation, recycling, and land memory: An integrated analysis. *Journal of Hydrometeorology*, *10*(1), 278–288. https://doi.org/10.1175/2008JHM1016.1

Gallego-Elvira, B., Taylor, C. M., Harris, P. P., Ghent, D., Veal, K. L., & Folwell, S. S. (2016). Global observational diagnosis of soil moisture control on the land surface energy balance. *Geophysical Research Letters*, *43*, 2623–2631. https://doi.org/10.1002/2016GL068178

Guo, Z., Dirmeyer, P. A., Koster, R. D., Sud, Y. C., Bonan, G., Oleson, K. W., et al. (2006). GLACE: The Global Land-Atmosphere Coupling Experiment. Part II: Analysis. *Journal of Hydrometeorology*, *7*, 611–625. https://doi.org/10.1175/JHM511.1

Huang, J., Yu, H., Guan, X., Wang, G., & Guo, R. (2016). Accelerated dryland expansion under climate change. *Nature Climate Change*, *6*(2), 166–171. https://doi.org/10.1038/nclimate2837

Koster, R. D., Dirmeyer, P. A., Guo, Z., Bonan, G., Chan, E., Cox, P., et al., & GLACE Team (2004). Regions of strong coupling between soil moisture and precipitation. *Science*, *305*(5687), 1138–1140. https://doi.org/10.1126/science.1100217

Koster, R. D., Sud, Y. C., Guo, Z., Dirmeyer, P. A., Bonan, G., Oleson, K. W., et al. (2006). GLACE: The Global Land–Atmosphere Coupling Experiment. Part I: Overview. *Journal of Hydrometeorology*, *7*(4), 590–610. https://doi.org/10.1175/JHM510.1

Lawrence, D. M., Thornton, P. E., Oleson, K. W., & Bonan, G. B. (2007). The partitioning of evapotranspiration into transpiration, soil evaporation, and canopy evaporation in a GCM: Impacts on land–atmosphere interaction. *Journal of Hydrometeorology*, *8*(4), 862–880. https://doi.org/10.1175/JHM596.1

Lian, X., Piao, S., Huntingford, C., Li, Y., Zeng, Z., Wang, X., et al. (2018). Partitioning global land evapotranspiration using CMIP5 models constrained by observations. *Nature Climate Change*, *8*(7), 640–646. https://doi.org/10.1038/s41558-018-0207-9

Miralles, D. G., Gash, J. H., Holmes, T. R., de Jeu, R. A., & Dolman, A. J. (2010). Global canopy interception from satellite observations. *Journal of Geophysical Research*, *115*, D16122. https://doi.org/10.1029/2009JD013530

Mueller, B., & Seneviratne, S. I. (2014). Systematic land climate and evapotranspiration biases in CMIP5 simulations. *Geophysical Research Letters*, *41*, 128–134. https://doi.org/10.1002/2013GL058055

Riahi, K., Rao, S., Krey, V., Cho, C., Chirkov, V., Fischer, G., et al. (2011). RCP 8.5—A scenario of comparatively high greenhouse gas emissions. *Climatic Change*, *109*(1-2), 33–57. https://doi.org/10.1007/s10584-011-0149-y

Santanello, J. A. Jr., Dirmeyer, P. A., Ferguson, C. R., Findell, K. L., Tawfik, A. B., Berg, A., et al. (2018). Land-atmosphere interactions: The LoCo perspective. *Bulletin of the American Meteorological Society*. https://doi.org/10.1175/BAMS-D-17-0001.1

Scheff, J., & Frierson, D. M. (2014). Scaling potential evapotranspiration with greenhouse warming. *Journal of Climate*, *27*(4), 1539–1558. https://doi.org/10.1175/JCLI-D-13-00233.1

Seneviratne, S. I., Corti, T., Davin, E. L., Hirschi, M., Jaeger, E. B., Lehner, I., et al. (2010). Investigating soil moisture–climate interactions in a changing climate: A review. *Earth-Science Reviews*, *99*(3-4), 125–161. https://doi.org/10.1016/j.earscirev.2010.02.004

Seneviratne, S. I., Lüthi, D., Litschi, M., & Schär, C. (2006). Land–atmosphere coupling and climate change in Europe. *Nature*, *443*(7108), 205–209. https://doi.org/10.1038/nature05095

Trugman, A. T., Medvigy, D., Mankin, J. S., & Anderegg, W. R. L. (2018). Soil moisture stress as a major driver of carbon cycle uncertainty. *Geophysical Research Letters*, *45*, 6495–6503. https://doi.org/10.1029/2018GL078131

Williams, I. N., Lu, Y., Kueppers, L. M., Riley, W. J., Biraud, S. C., Bagley, J. E., & Torn, M. S. (2016). Land-atmosphere coupling and climate prediction over the US Southern Great Plains. *Journal of Geophysical Research: Atmospheres*, *121*, 12,125–12,144. https://doi.org/10.1002/2016JD025223

Zhao, T., & Dai, A. (2015). The magnitude and causes of global drought changes in the twenty-first century under a low–moderate emissions scenario. *Journal of Climate*, *28*(11), 4490–4512. https://doi.org/10.1175/JCLI-D-14-00363.1